Theoretical Investigation of Hydrogen Bonds between CO and HNF_2, H_2NF, and HNO†

An Yong Li*

School of Chemistry and Chemical Engineering, Southwestern University, 400715, ChongQing, P R China

Received: April 13, 2006; In Final Form: July 5, 2006

Ab initio quantum mechanics methods were applied to investigate the hydrogen bonds between CO and HNF_2, H_2NF, and HNO. We use the Hartree−Fock, MP2, and MP4(SDQ) theories with three basis sets 6-311++G(d,p), 6-311++G(2df,2p), and AUG-cc-pVDZ, and both the standard gradient and counterpoise-corrected gradient techniques to optimize the geometries in order to explore the effects of the theories, basis sets, and different optimization methods on this type of H bond. Eight complexes are obtained, including the two types of C···H−N and O···H−N hydrogen bonds: OC···HNF_2(C_s), OC···H_2NF(C_s and C_1), and OC···HNO(C_s), and CO···HNF_2(C_s), CO···H_2NF(C_s and C_1), and CO···HNO(C_s). The vibrational analysis shows that they have no imaginary frequencies and are minima in potential energy surfaces. The N−H bonds exhibit a small decrease with a concomitant blue shift of the N−H stretch frequency on complexation, except for OC···HNF_2 and OC···H_2NF(C_1), which are red-shifting at high levels of theory and with large basis sets. The O···H−N hydrogen bonds are very weak, with 0 K dissociation energies of only 0.2−2.5 kJ/mol, but the C···H−N hydrogen bonds are stronger with dissociation energies of 2.7−7.0 kJ/mol at the MP2/AUG-cc-pVDZ level. It is notable that the IR intensity of the N−H stretch vibration decreases on complexation for the proton donor HNO but increases for HNF_2 and H_2NF. A calculation investigation of the dipole moment derivative leads to the conclusion that a negative permanent dipole moment derivative of the proton donor is not a necessary condition for the formation of the blue-shifting hydrogen bond. Natural bond orbital analysis shows that for the C···H−N hydrogen bonds a large electron density is transferred from CO to the donors, but for the O···H−N hydrogen bonds a small electron density transfer exists from the proton donor to the acceptor CO, which is unusual except for CO···H_2NF(C_s). From the fact that the bent hydrogen bonds in OC(CO)···H_2NF(C_s) are quite different from those in the others, we conclude that a greatly bent H-bond configuration shall inhibit both hyperconjugation and rehybridization.

1. Introduction

Hydrogen bonding is very important for many chemical and biochemical processes.[1−3] Classical H bonds are of the X−H···Y type with X and Y electronegative atoms, or Y being π-electron systems. These H bonds are characterized by elongation of the X−H bond and a concomitant decrease of the X−H stretch frequency (red shift), and also usually an increase of the IR intensity of the X−H stretch vibration upon formation of the complex. Another kind of hydrogen bond, named improper blue-shifted hydrogen bonds, have been reported by a lot of experimental[4−8] and theoretical[9,10] investigations, which have the structure XC−H···Y with Y an electronegative atom or π-electron group, and carbon often bonded to an electronegative atom X. This H bond is characterized by contraction of the C−H bond and a concomitant increase of the C−H stretch frequency (blue shift) on complexation. Concerning the intrinsic origin of the H bonds, natural bond orbital (NBO) analysis finds that for the classical red-shifting H bond, electron density transfer (EDT) exists from the lone electron pair or π electrons of the proton acceptor Y to the σ*(X−H) antibonding orbital of the proton donor; the increase of electron density in the σ* antibonding orbital causes weakening of the X−H bond and its elongation and red shift of the X−H stretch frequency. For the improper blue-shifted H bond, however, systematical investigation by Hobza and co-workers[11] found that the main part of the electron density is transferred not to the σ*(C−H) antibonding orbital but to the lone pairs of the X atom or the σ*(X−C) antibonding orbital, which first causes structural reorganization of the proton donor and, subsequently, contraction of the C−H bond and blue shift of the C−H stretch frequency. The standard red-shifted hydrogen bond usually has a larger EDT and a higher interaction energy than the improper blue-shifted hydrogen bond.

In addition to the fact that the C−H bond can act as the proton donor to form blue-shifting H bonds, theoretical studies[12,13] have shown that other X−H bonds such as N−H, P−H, Si−H, and so forth can also act as proton donors to form blue-shifting H bonds. The N−H···Y hydrogen bonds have many properties similar to the C−H···Y H bonds. Because nitrogen is more electronegative than carbon and the σ*(N−H) orbital is a better electron acceptor than the σ*(C−H) orbital, the N−H···Y blue-shifted H bonds have some properties different from those of the C−H···Y blue-shifted H bonds. In this article, we apply the Hartree−Fock, MP2, and MP4(SDQ) methods with the 6-311++G(d,p), 6-311++G(2df,2p), and AUG-cc-pVDZ basis sets to study the H bonds between CO and HNF_2, H_2NF, and HNO. Because the dipole moment of the proton acceptor CO is quite small, only about 0.12 Debye experimentally,[14] pointing from carbon (the negative end) to oxygen (the positive end), although the dipole moment direction of CO is theoretically reversed, both carbon and oxygen can interact with the proton donor to form H bonds. Our calculation shows that these two types of H bonds indeed exist: C···HN and O···HN. The interaction energies, vibrational frequencies, and IR intensities

* E-mail: aylifnsy@swnu.edu.cn.

† Supported by Natural Science Foundation of Chongqing, P R China.

10.1021/jp062291p CCC: $33.50
Published on Web 08/26/2006

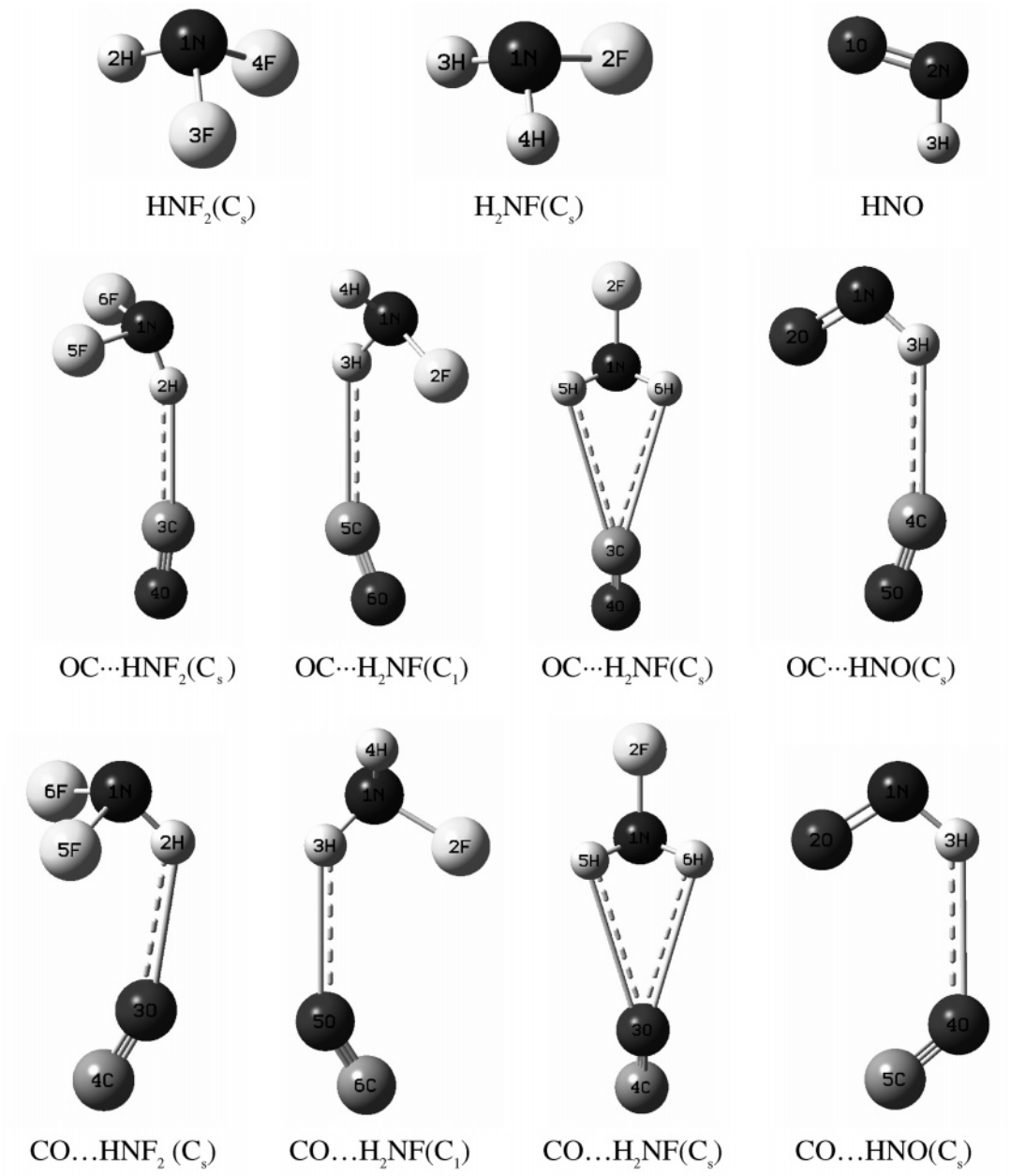

Figure 1. Geometries of the monomers and complexes with their symmetries in parentheses.

are computed. The NBO method is applied to analyze the electron density transfer between the proton acceptor and donor and to investigate the origin of the H bonds. In the following sections, we shall give our computational details and results.

2. Computational Methods

All of the calculations in this article were performed using the Gaussian 03 program.[15] The geometries of the monomers and the complexes were optimized at the HF/6-311++G(d,p), MP2/6-311++G(d,p), MP2/6-311++G(2df,2p), MP2/AUG-cc-pVDZ, and MP4(SDQ)/6-311++G(d,p) levels to explore the effects of the theories and basis sets. Both the standard gradient and counterpoise (CP)-corrected gradient techniques were applied to optimize the geometries of the complexes for the purpose of exploring their differences in explaining the H-bonding interaction. Eight complexes are found, OC···HNF_2(C_s), OC···H_2NF(C_s and C_1), and OC···HNO(C_s), and CO···HNF_2(C_s), CO···H_2NF(C_s and C_1), and CO···HNO(C_s), the vibrational analysis shows that they have no imaginary frequencies and are all minima in the potential energy surfaces (PESs). The geometries of all of the monomers and complexes are shown in Figure 1. The structure parameters of the monomers and the C···HN and O···HN complexes are listed in Table 1a, b, and c, respectively.

The interaction energies were determined and corrected for the zero-point vibrational energy (ZPE) at all of the above theoretical levels for the C···HN and O···HN complexes. The corrections for the basis set superposition error (BSSE) were computed using the function counterpoise (CP) procedure proposed by Boys and Bernardi[16] on both the standard and CP-corrected PESs at all of the theoretical levels. The formula is as follows:

$$\delta_{AB}^{BSSE} = E_{AB}^{A}(A) + E_{AB}^{B}(B) - E_{AB}^{AB}(A) - E_{AB}^{AB}(B) \quad (1)$$

Here $E_Y^X(Z)$ represents the energy of system Z at geometry Y with basis set X. In Table 2a and b, for the C···HN and O···HN complexes, respectively, we list the following: (1) The interac-

TABLE 1

(a) Geometry parameters of the monomers. NH, HNF, and HNFH represent bond length, bond angle, and dihedral angle, respectively (in units of angstroms and degrees). The values in parentheses are parameters optimized by the CP-corrected gradient technique

systems	parameters	HF 6-311++G(d,p)	MP2 6-311++G(d,p)	MP2 6-311++G(2df,2p)	MP2 AUG-cc-PVDZ	MP4(SDQ) 6-311++G(d,p)
CO	CO	1.1053	1.1400	1.1367	1.1502	1.1359
HNF_2 (C_s)	NH	1.0054	1.0260	1.0225	1.0326	1.0268
	NF	1.3434	1.3918	1.3890	1.4111	1.3899
	HNF	102.4	100.4	100.2	99.3	100.6
	FNF	103.8	103.7	103.5	103.1	103.4
H_2NF (C_s)	NH	1.0029	1.0202	1.0165	1.0268	1.0211
	NF	1.3759	1.4197	1.4179	1.4412	1.4200
	HNH	107.1	105.4	105.4	104.6	105.3
	HNF	103.3	102.1	101.8	100.9	102.0
	HNFH	111.5	108.9	108.7	107.4	108.7
HNO	NH	1.0323	1.0542	1.0494	1.0596	1.0577
	NO	1.1670	1.2213	1.2196	1.2326	1.2090
	HNO	109.4	107.9	107.9	107.4	108.4

(b) Geometry parameters of the four complexes: OC···HNF_2(C_s), OC···H_2NF(C_s and C_1), and OC···HNO(C_s)

systems	parameters	HF 6-311++G(d,p)	MP2 6-311++G(d,p)	MP2 6-311++G(2df,2p)	MP2 AUG-cc-pVDZ	MP4(SDQ) 6-311++G(d,p)
OC···HNF_2(C_s)	NH	1.0051(1.0052)	1.026(1.0262)	1.0233(1.0231)	1.0329(1.0332)	1.0262(1.0266)
	NF	1.3449(1.3446)	1.3945(1.3941)	1.3921(1.3916)	1.4142(1.4136)	1.3921(1.3919)
	OC	1.1034(1.1034)	1.1381(1.1382)	1.1346(1.1348)	1.1482(1.1483)	1.1338(1.1340)
	C···H	2.653(2.7174)	2.3903(2.4696)	2.3193(2.3958)	2.3284(2.4262)	2.4404(2.5290)
	CHN	153.1(153.8)	160.7(166.4)	157.7(160.7)	157.9(154.1)	160.5(160.7)
	OCH	174.1(174.1)	174.2(175)	173.8(173.3)	172.6(170.9)	174.3(174.3)
	HNF	102.2(102.3)	100.1(100.2)	99.7(99.8)	98.9(99.0)	100.3(100.4)
	FNHF	107.2(107.2)	105.9(106.0)	105.5(105.6)	104.7(104.7)	105.7(105.8)
OC···H_2NF(C_1)	NH	1.0029(1.0029)	1.0204(1.0203)	1.0172(1.0171)	1.0271(1.0273)	1.0216(1.0211)
	NF	1.3774(1.3773)	1.4220(1.4218)	1.4204(1.4198)	1.4439(1.4434)	1.4228(1.4217)
	OC	1.1044(1.1043)	1.1389(1.1389)	1.1354(1.1356)	1.1491(1.1491)	1.1346(1.1347)
	C···H	2.8494(2.8994)	2.5774(2.6449)	2.4994(2.5855)	2.5090(2.6089)	2.6232(2.6968)
	CHN	136.7(139.4)	137.7(147.6)	137.9(138.0)	139.0(137.3)	137.1(144.3)
	OCH	161.5(160.4)	157.5(161.6)	158.4(157.5)	158.5(155.7)	157.8(161.7)
	HNF	103.1(103.2)	101.8(101.8)	101.4(101.5)	100.5(100.6)	101.7(101.8)
	HNFH	111.5(111.5)	108.9(109.1)	108.8(108.8)	107.5(107.5)	108.6(108.8)
OC···H_2NF(C_s)	NH	1.0027(1.0027)	1.0200(1.0200)	1.0163(1.0163)	1.0266(1.0266)	1.0208(1.0208)
	NF	1.3766(1.3763)	1.4219(1.4213)	1.4197(1.4190)	1.4431(1.4430)	1.4216(1.4210)
	OC	1.1043(1.1042)	1.1391(1.1390)	1.1357(1.1358)	1.1493(1.1493)	1.1348(1.1348)
	C···H	3.2541(3.3319)	2.9173(3.0198)	2.8867(2.9573)	2.8740(2.9688)	2.9669(3.0784)
	CHN	94.1(95.1)	90.8(91.8)	89.7(90.6)	87.4(89.1)	90.6(91.8)
	OCH	156.3(156.5)	152.5(152.3)	152.7(152.2)	151.9(151.9)	152.7(152.7)
	HNF	103.4(103.4)	102.3(102.3)	102.1(102.1)	101.1(101.1)	102.2(102.2)
	HNFH	111.2(111.3)	108.3(108.5)	108.2(108.3)	106.9(106.9)	108.2(108.3)
O^aC···HNO^b(C_s)	NH	1.0310(1.0310)	1.0526(1.0528)	1.0485(1.0483)	1.0584(1.0587)	1.0558
	NO^b	1.1679(1.1679)	1.2224(1.2221)	1.2209(1.2208)	1.2335(1.2334)	1.2101
	O^aC	1.1043(1.1043)	1.1391(1.1390)	1.1358(1.1357)	1.1493(1.1493)	1.1349
	C···H	2.8618(2.8981)	2.5799(2.6641)	2.4947(2.5634)	2.5125(2.5992)	2.6442
	CHN	129.6(130.7)	127.9(130.2)	128.1(128.8)	127.5(127.6)	127.1
	O^aCH	164.1(163.5)	161.8(160.8)	162.5(161.0)	161.0(158.9)	161.9
	HNO^b	109.2(109.2)	107.5(107.6)	107.3(107.4)	106.8(107.0)	108.1

(c) geometry parameters of the four complexes: CO···HNF_2(C_s), CO···H_2NF(C_s and C_1), and CO···HNO(C_s)

systems	parameters	HF 6-311++G(d,p)	MP2 6-311++G(d,p)	MP2 6-311++G(2df,2p)	MP2 AUG-cc-PVDZ	MP4(SDQ) 6-311++G(d,p)
CO···HNF_2(C_s)	NH	1.0047(1.0049)	1.0256(1.0255)	1.0222(1.0222)	1.0321(1.0324)	1.0261
	NF	1.3447(1.3445)	1.3924(1.3924)	1.3897(1.3896)	1.4118(1.4117)	1.3908
	OC	1.1072(1.1072)	1.1408(1.1407)	1.1373(1.1373)	1.1505(1.1507)	1.1371
	O···H	2.4232(2.4599)	2.4623(2.5062)	2.4221(2.4891)	2.3713(2.4751)	2.4389
	OHN	168.6(177.4)	126.2(143.5)	128.3(135.2)	130.4(132.9)	128.5
	COH	173.2(175.1)	148.6(166)	158.4(160)	149.1(157.5)	148.1
	FNH	102.4(102.4)	100.2(100.3)	100.0(100)	99.1(99.2)	100.4
	FNHF	107.4(107.4)	106.0(106.1)	105.6(105.7)	104.8(104.9)	105.8
CO···H_2NF(C_1)	NH	1.0028(1.0028)	1.0202(1.0201)	1.0166(1.0165)	1.0265(1.0268)	
	NF	1.3775(1.3773)	1.4203(1.4201)	1.4184(1.4182)	1.4417(1.4416)	
	OC	1.1066(1.1065)	1.1404(1.1404)	1.1371(1.1370)	1.1503(1.1505)	
	O···H	2.6110(2.6446)	2.5735(2.6261)	2.4975(2.5947)	2.4994(2.6082)	
	OHN	140.3(143.4)	120.6(134.5)	129.8(129.3)	121.8(125.1)	
	COH	137.7(139.8)	140.0(150.9)	146.5(143.9)	137.6(140)	
	HNF	103.2(103.2)	102.1(102.0)	101.7(101.8)	100.8(100.9)	
	HNFH	111.5(111.5)	108.9(109.1)	108.8(108.9)	107.6(107.5)	

TABLE 1 (Continued)

systems	parameters	HF 6-311++G(d,p)	MP2 6-311++G(d,p)	MP2 6-311++G(2df,2p)	MP2 AUG-cc-PVDZ	MP4(SDQ) 6-311++G(d,p)
CO···$H_2NF(C_s)$	NH	1.0025(1.0026)	1.0201(1.0200)	1.0164(1.0165)	1.0267(1.0267)	
	NF	1.3771(1.3769)	1.4201(1.4197)	1.4181(1.4178)	1.4410(1.4411)	
	OC	1.1066(1.1065)	1.1406(1.1405)	1.1372(1.1372)	1.1505(1.1507)	
	O···H	2.9292(3.0149)	2.7927(2.9631)	2.8021(2.8878)	2.7546(2.8934)	
	OHN	100.9(100.1)	91.3(92.9)	90.3(91.4)	88.4(89.8)	
	CON	157.1(152.5)	139.4(145.2)	140.8(140.2)	141.5(137.6)	
	HNF	103.4(103.4)	102.2(102.2)	101.9(101.9)	101.0(101.0)	
	HNFH	111.1(111.2)	108.6(108.7)	108.5(108.5)	107.2(107.2)	
CO···HNO(C_s)	NH	1.0308(1.0309)	1.0531(1.0532)	1.0490(1.0488)	1.0589(1.0592)	1.0561
	NO	1.1680(1.1678)	1.2217(1.2216)	1.2198(1.2198)	1.2326(1.2326)	1.2097
	OC	1.1066(1.1065)	1.1404(1.1403)	1.1374(1.1371)	1.1508(1.1507)	1.1367
	O···H	2.6591(2.6985)	2.5787(2.7175)	2.5256(2.6290)	2.4908(2.6142)	2.5804
	OHN	134.7(136.0)	128.7(131.7)	130.6(130.5)	132.1(130.8)	129.3
	COH	142.0(142.5)	146.7(155.3)	130.0(141.3)	125.8(130.5)	139.2
	HNO	109.3(109.3)	107.8(107.8)	107.8(107.8)	107.3(107.3)	108.3

tion energies: $\delta E = E(\mathrm{AB})^{\mathrm{standard}} - E(\mathrm{A}) - E(\mathrm{B}) + \delta(\mathrm{BSSE})$ and $\delta E^{\mathrm{CP}} = E(\mathrm{AB})^{\mathrm{CP}} - E(\mathrm{A}) - E(\mathrm{B})$, computed by the standard gradient and the CP−corrected gradient techniques, respectively, where $E(\mathrm{AB})^{\mathrm{standard}}$ is the energy of the complex on the standard PES without BSSE correction and $E(\mathrm{AB})^{\mathrm{CP}}$ on the CP-corrected PES with BSSE correction; (2) $\delta(\mathrm{BSSE})$ and $\delta(\mathrm{BSSE})^{\mathrm{CP}}$, $\delta(\mathrm{ZPE})$ and $\delta(\mathrm{ZPE})^{\mathrm{CP}}$: the BSSE corrections for the energy and the ZPE corrections, computed by the standard gradient and CP-corrected gradient methods, respectively; (3) $D_0 = -E - \delta(\mathrm{ZPE})$, $D_0^{\mathrm{CP}} = -E^{\mathrm{CP}} - \delta(\mathrm{ZPE})^{\mathrm{CP}}$: the 0 K dissociation energies of the complexes computed by the two gradient optimization methods, respectively.

We performed the vibrational analysis calculation for the monomers and complexes at all of the optimized geometries. The vibrational harmonic frequencies and IR intensities of the various intramolecular vibration modes were obtained. The results are shown in Table 3a and b for the C···HN and O··· HN complexes, respectively.

By using the GenNBO5.0W program,[17] we have also performed the NBO calculation for all of the monomers and the complexes. Comparing the results of the complex with those of the monomers, we obtain the electron density transfer (EDT) between the proton acceptor and donor, the variations of occupancies of various natural bond orbitals such as σ(N−H), σ^*(N−H), σ^*(N−X), and Lp(X = F,O) of the donor and Lp(O,C) of CO, the change in the *s* character of the nitrogen's sp^n hybrids of the σ(N−H) bond, and the variation of the natural atomic charges at various atoms upon the formation of the H bonds. All of the results of NBO analysis are listed in Table 4.

3. Results and Discussions

3.1. Geometry Parameters and Interaction Energies. Table 1a shows that the three theoretical levels, MP2/6-311++G(d,p), MP2/6-311++G(2df,2p), and MP4(SDQ)/6-311++G(d,p), predict similar geometry structures of the monomers. However, the Hartree−Fock theory produces shorter bond lengths and larger bond angles and dihedral angles; in contrast, the MP2/AUG-cc-pVDZ level of theory predicts longer bonds and smaller angles. These properties also occur for the intramolecular geometry parameters of the optimized complexes as shown in Table 1b and c, regardless of whether we use the standard or CP-corrected gradient optimization techniques. The interaction distance C(O)···H and the relative orientation (∠C(O)HN) between the monomers on complexation are sensitive to the theories and basis sets, but the variation trend of the intramolecular geometry parameters on complexation is consistent at all of the theoretical levels (except for OC···HNF_2 and OC···$H_2NF(C_1)$), as shown in Table 1b and c. The different gradient optimization techniques have little effect on the intramolecular geometry parameters, but large influences on the intermolecular parameters that the CP-corrected gradient method enlarges the C(O)···H distance and the C(O)···H−N angle, δ(C···H) = 0.07−0.1 Å, δ(CHN) = 1−10°, and δ(O···H) = 0.04−0.17 Å, δ(OHN) = 1.6−17° at the MP2/6-311++G(d,p) level. This implies that in the supermolecule method of molecular interaction the superposition of the basis sets of two monomers, and therefore the superposition of their molecular orbitals, strengthens the attractive interaction between the monomers and makes them approaching, and that the CP-corrected gradient technique corrects this error in some extent, increasing the interaction distance and making the H bond more collinear. This property is consistent with the BSSE incorrectly lowering the energy of the complex and increasing the interaction energy. In these eight complexes, the H bond C(O)···H−N is not linear at all of the theoretical levels.

The experimental value[18] of the bond length of CO is 1.1281 Å. The geometry parameters[19] of the C_s symmetry HNF_2 are r(N−F) = 1.400 ± 0.002 Å, r(N−H) = 1.026 ± 0.002 (Å), FNF = 101.9 ± 0.2° and HNF = 99.8 ± 0.2°. Table 1a shows that all of these levels of theory are not very good for predicting the bond length of CO, of which the MP4(SDQ) method and the 6-311++G(2df,2p) basis set seem a little better, and that the MP2 method with the 6-311++G(d,p) and AUG-cc-pVDZ basis sets overestimates it and the HF/6-311++G(d,p) level underestimates it. For HNF_2, all of the methods overestimate the bond angles; the bond lengths predicted by the MP2 and MP4(SDQ) methods with the 6-311++G(d,p) basis set agree better with the experimental values than the others. Similarly, the MP2/AUG-cc- pVDZ method overestimates and the HF/6-311++G(d,p) method underestimates the bond lengths. So the MP*n* methods with the basis set 6-311G plus polarized and diffuse functions are preferable for predicting reliable geometry parameters; at an expense of not very large CPU time, the MP2/6-311++G(d,p) method is reliable for predicting geometry.

From Table 2, we see that the four O···H−N H bonds are very weak, their interaction energies are less than 5 kJ/mol at all of the theoretical levels, the dissociation energies are 0.2∼2.5kJ/mol at the MP2/AUG-cc-pVDZ level, and the C···H−N H bonds are stronger than the O···H−N H bonds; their interaction energies are 6−10 kJ/mol and the dissociation energies are 2−7 kJ/mol at the MP2/AUG-cc-pVDZ level, two or three times larger than those of the corresponding O···H−N complexes. From Table 2a and b, it is found that different theories and basis sets have important effects on the interaction

TABLE 2

(a) Interaction energies, ZPE, and BSSE corrections (in units of kJ/mol) of the four complexes: $OC\cdots HNF_2(C_s)$, $OC\cdots H_2NF(C_s$ and $C_1)$, and $OC\cdots HNO(C_s)$

systems	properties	HF 6-311++G(d,p)	MP2 6-311++G(d,p)	MP2 6-311++G(2df,2p)	MP2 aug-cc-pvdz	MP4(SDQ) 6-311++G(2df,2p)
$OC\cdots HNF_2$	δE	−4.80	−8.86	−9.49	−9.43	−7.55
	δE^{CP}	−4.84	−9.00	−9.64	−9.63	−7.68
	δ(BSSE)	1.13	2.74	2.84	4.12	2.62
	$\delta(BSSE)^{CP}$	1.04	2.44	2.54	3.72	2.35
	δ(ZPE)	2.38	2.77	2.91	2.96	2.62
	$\delta(ZPE)^{CP}$	2.28	2.55	2.67	2.59	2.48
	D_0	2.41	6.08	6.58	6.47	4.93
	D_0^{CP}	2.56	6.45	6.98	7.03	5.20
$OC\cdots H_2NF(C_1)$	δE	−2.98	−5.54	−6.25	−6.33	−4.85
	δE^{CP}	−3.03	−5.75	−6.37	−6.48	−5.03
	δ(BSSE)	0.89	2.26	2.02	3.00	2.20
	$\delta(BSSE)^{CP}$	0.79	1.82	1.79	2.71	1.80
	δ(ZPE)	2.42	2.82	3.04	2.93	2.79
	$\delta(ZPE)^{CP}$	2.26	2.60	2.77	2.69	2.52
	D_0	0.56	2.72	3.21	3.40	2.06
	D_0^{CP}	0.77	3.15	3.60	3.78	2.51
$OC\cdots H_2NF(C_s)$	δE	−2.27	−5.40	−5.86	−6.03	−4.49
	δE^{CP}	−2.30	−5.54	−5.94	−6.22	−4.64
	δ(BSSE)	0.88	2.50	2.00	3.24	2.40
	$\delta(BSSE)^{CP}$	0.82	2.19	1.83	2.85	2.08
	δ(ZPE)	1.78	2.53	2.43	2.66	2.43
	$\delta(ZPE)^{CP}$	1.50	2.08	2.16	2.21	1.96
	D_0	0.49	2.87	3.42	3.37	2.05
	D_0^{CP}	0.81	3.46	3.78	4.01	2.68
$OC\cdots HNO$	δE	−2.98	−5.67	−6.89	−6.91	−4.78
	δE^{CP}	−2.99	−5.83	−6.99	−7.04	
	δ(BSSE)	0.87	2.47	2.06	2.94	2.27
	$\delta(BSSE)^{CP}$	0.83	2.15	1.86	2.67	
	δ(ZPE)	3.05	3.75	4.28	4.14	3.58
	$\delta(ZPE)^{CP}$	2.96	3.50	3.90	3.78	
	D_0	−0.07	1.92	2.61	2.77	1.20
	D_0^{CP}	0.03	2.33	3.09	3.26	

(b) Interaction energies, ZPE, and BSSE corrections (in units of kJ/mol) of the four complexes: $CO\cdots HNF_2(C_s)$, $CO\cdots H_2NF(C_s$ and $C_1)$, and $CO\cdots HNO(C_s)$

systems	properties	HF 6-311++G(d,p)	MP2 6-311++G(d,p)	MP2 6-311++G(2df,2p)	MP2 aug-cc-pvdz	MP4(SDQ) 6-311++G(d,p)
$CO\cdots HNF_2$	δE	−4.90	−2.58	−3.54	−3.95	−3.35
	δE^{CP}	−4.94	−3.33	−3.78	−4.23	
	δ(BSSE)	1.12	3.89	2.92	3.19	3.71
	$\delta(BSSE)^{CP}$	1.04	2.52	2.43	2.62	
	δ(ZPE)	1.57	1.97	1.92	2.07	1.98
	$\delta(ZPE)^{CP}$	1.54	1.60	1.62	1.68	
	D_0	3.32	0.62	1.62	1.88	1.37
	D_0^{CP}	3.40	1.74	2.16	2.55	
$CO\cdots H_2NF(C_1)$	δE	−3.10	−2.21	−2.93	−3.24	
	δE^{CP}	−3.14	−2.62	−3.07	−3.43	
	δ(BSSE)	0.97	3.30	2.09	2.60	
	$\delta(BSSE)^{CP}$	0.90	2.40	1.82	2.20	
	δ(ZPE)	1.94	1.95	1.87	2.11	
	$\delta(ZPE)^{CP}$	1.77	1.70	1.66	1.64	
	D_0	1.16	0.26	1.07	1.13	
	D_0^{CP}	1.37	0.93	1.41	1.79	
$CO\cdots H_2NF(C_s)$	δE	−2.75	−1.88	−2.58	−2.72	
	δE^{CP}	−2.80	−2.18	−2.67	−2.99	
	δ(BSSE)	0.99	2.86	2.16	2.48	
	$\delta(BSSE)^{CP}$	0.88	2.27	1.96	1.94	
	δ(ZPE)	1.38	1.87	1.75	1.91	
	$\delta(ZPE)^{CP}$	1.19	1.34	1.44	1.45	
	D_0	1.38	0.01	0.83	0.81	
	D_0^{CP}	1.62	0.84	1.23	1.54	
$CO\cdots HNO$	δE	−2.87	−1.75	−2.60	−2.93	−2.18
	δE^{CP}	−2.88	−2.04	−2.72	−3.07	
	δ(BSSE)	0.84	2.99	1.93	2.25	2.82
	$\delta(BSSE)^{CP}$	0.81	2.35	1.72	1.97	
	δ(ZPE)	2.28	2.15	2.39	2.71	2.43
	$\delta(ZPE)^{CP}$	2.17	1.85	1.97	2.14	
	D_0	0.58	−0.40	0.21	0.22	−0.26
	D_0^{CP}	0.72	0.19	0.75	0.93	

TABLE 3

(a) Harmonic frequencies of the NH and CO stretch vibrations in the monomers, frequency shifts and variation of bond lengths upon formation of the C···H–N complexes. δr(NH), $\delta \nu$(NH), $\delta r(\mathrm{NH})^{\mathrm{CP}}$, $\delta \nu(\mathrm{NH})^{\mathrm{CP}}$ are variations of the N-H bond length and stretch frequency, computed by the standard and CP-corrected gradient techniques respectively. The values in the parentheses are IR intensities of the NH and CO stretch vibrational modes.

Systems	Properties	HF	MP2			MP4(SDQ)
		6-311++G(d,p)	6-311++G(d,p)	6-311++G(2df,2p)	AUG-cc-PVDZ	6-311++G(d,p)
CO	ν(CO)	2432(163)	2124(37)	2127(36)	2072(34)	2147(63)
HNF_2	ν(NH)	3708(7)	3444(2)	3446(4)	3407(3)	3427(0.4)
OC…$HNF_2(C_s)$	δr(NH)	**-0.0003**	**0**	+0.0008	+0.0003	**-0.0006**
	$\delta \nu$(NH)	**+12(34)**	**+10(61)**	-3(86)	0(81)	**+22(39)**
	δr(OC)	**−0.0019**	**−0.0019**	**-0.0021**	**−0.0020**	**-0.0021**
	$\delta \nu$(CO)	**+19(158)**	**+15(28)**	**+17(28)**	**+17(27)**	**+16(54)**
	$\delta r(\mathrm{NH})^{\mathrm{CP}}$	**-0.0002**	+0.0002	+0.0006	+0.0006	**-0.0002**
	$\delta \nu(\mathrm{NH})^{\mathrm{CP}}$	**+9(31)**	**+7(52)**	0(72)	-1(56)	**+16(29)**
H_2NF	$\nu(\mathrm{NH})_s$	3697(0.7)	3477(0.4)	3482(0.3)	3434(1)	3464(1)
	$\nu(\mathrm{NH})_a$	3790(7)	3587(3)	3588(8)	3547(5)	3563(1)
OC···H_2NF(C1)	δr(NH)	**0**	+0.0002	+0.0007	+0.0003	+0.0005
	$\delta \nu(\mathrm{NH})_s$	**+3(3)**	**+1(5)**	-3(9)	0(8)	-2(3)
	$\delta \nu(\mathrm{NH})_a$	**+3(14)**	**0(15)**	-4(25)	0(21)	-4(7)
	δr(OC)	**−0.0010**	**−0.0011**	**-0.0013**	**−0.0011**	**-0.0013**
	$\delta \nu$(CO)	**+10(164)**	**+9(33)**	**+11(33)**	**+10(31)**	**+10(59)**
	$\delta r(\mathrm{NH})^{\mathrm{CP}}$	**0**	+0.0001	+0.0006	+0.0005	**0**
	$\delta \nu(\mathrm{NH})_s^{\mathrm{CP}}$	**+2(3)**	**+2(6)**	-1(7)	-1(6)	**+4(3)**
	$\delta \nu(\mathrm{NH})_a^{\mathrm{CP}}$	**+2(14)**	**+1(16)**	-2(22)	-2(17)	**+3(7)**
OC···H_2NF(Cs)	δr(NH)	**−0.0002**	**−0.0002**	**-0.0002**	**−0.0002**	**-0.0003**
	$\delta \nu(\mathrm{NH})_s$	**+6(1)**	**+9(1)**	**+7(1)**	**+7(2)**	**+8(1)**
	$\delta \nu(\mathrm{NH})_a$	**+5(7)**	**+6(4)**	**+5(9)**	**+5(6)**	**+7(1)**
	δr(OC)	**−0.0010**	**−0.0009**	**-0.0010**	**−0.0009**	**-0.0011**
	$\delta \nu$(CO)	**+10(166)**	**+6(35)**	**+7(36)**	**+8(35)**	**+8(62)**
	$\delta r(\mathrm{NH})^{\mathrm{CP}}$	**-0.0002**	**-0.0002**	**-0.0002**	**-0.0002**	**-0.0003**
	$\delta \nu(\mathrm{NH})_s^{\mathrm{CP}}$	**+6(1)**	**+8(1)**	**+7(1)**	**+7(2)**	**+7(1)**
	$\delta \nu(\mathrm{NH})_a^{\mathrm{CP}}$	**+5(7)**	**+6(4)**	**+5(8)**	**+5(6)**	**+5(1)**
HNO	ν(NH)	3319(59)	3034(120)	3043(95)	3006(106)	2978(139)
OC···HNO(Cs)	δr(NH)	**−0.0013**	**−0.0016**	**-0.0009**	**−0.0012**	**-0.0019**
	$\delta \nu$(NH)	**+29(32)**	**+39(54)**	**+32(36)**	**+34(44)**	**44(74)**
	δr(OC)	**−0.0010**	**−0.0009**	**-0.0009**	**−0.0009**	**-0.0010**
	$\delta \nu$(CO)	**+10(163)**	**+7(34)**	**+7(34)**	**+9(33)**	**+7(61)**
	$\delta r(\mathrm{NH})^{\mathrm{CP}}$	**-0.0013**	**-0.0014**	**-0.0011**	**-0.0009**	**-0.0013**
	$\delta \nu(\mathrm{NH})^{\mathrm{CP}}$	**+27(33)**	**+36(59)**	**+34(40)**	**+30(50)**	**+32(86)**

(b) Shifts of harmonic frequencies and variation of bond lengths of the NH and CO upon formation of the O···H–N complexes. Notes: [a] asymmetrical N-H stretch vibration; [s] symmetrical N-H stretch vibration.

Systems	Properties	HF	MP2			MP4(SDQ)
		6-311++G(d,p)	6-311++G(d,p)	6-311++G(2df,2p)	AUG-cc-PVDZ	6-311++G(d,p)
CO…HNF_2	δr(NH)	-0.0007	-0.0004	-0.0003	-0.0005	-0.0007
	$\delta \nu$(NH)	22(36)	13(7)	12(13)	14(12)	20(5)
	δr(OC)	0.0019	0.0008	0.0006	0.0003	0.0012
	$\delta \nu$(CO)	-18(206)	-3(49)	-2(49)	0(48)	-7(77)
	$\delta r(\mathrm{NH})^{\mathrm{CP}}$	-0.0005	-0.0005	-0.0003	-0.0002	
	$\delta \nu(\mathrm{NH})^{\mathrm{CP}}$	19(35)	16(11)	11(14)	10(11)	

TABLE 3 (Continued)

Systems	Properties	HF	MP2			MP4(SDQ)
		6-311++G(d,p)	6-311++G(d,p)	6-311++G(2df,2p)	AUG-cc-PVDZ	6-311++G(d,p)
CO···$H_2NF(C_1)$	δr(NH)	-0.0001	0.0000	0.0001	-0.0003	
	$\delta\nu(NH)_s$	5(2)	1(1)	2(1)	3(2)	
	$\delta\nu(NH)_a$	4(14)	0(5)	1(13)	4(8)	
	δr(OC)	0.0013	0.0004	0.0004	0.0001	
	$\delta\nu$(CO)	-12(178)	-1(44)	-1(45)	1(42)	
	$\delta r(NH)^{CP}$	-0.0001	-0.0001	0.0000	0.0000	
	$\delta\nu(NH)_s^{CP}$	4(3)	3(1)	2(1)	1(2)	
	$\delta\nu(NH)_a^{CP}$	4(14)	3(7)	2(12)	1(8)	
CO···$H_2NF(C_s)$	δr(NH)	-0.0004	-0.0001	-0.0001	-0.0001	
	$\delta\nu(NH)_s$	9(1)	5(1)	3(1)	4(2)	
	$\delta\nu(NH)_a$	8(8)	4(4)	3(8)	3(5)	
	δr(OC)	0.0013	0.0006	0.0005	0.0003	
	$\delta\nu$(CO)	-12(191)	-2(48)	-2(46)	0(46)	
	$\delta r(NH)^{CP}$	-0.0003	-0.0002	0.0000	-0.0001	
	$\delta\nu(NH)_s^{CP}$	7(1)	4(1)	3(1)	3(2)	
	$\delta\nu(NH)_a^{CP}$	6(7)	3(4)	2(8)	2(5)	
CO···HNO	δr(NH)	-0.0015	-0.0011	-0.0004	-0.0007	-0.0016
	$\delta\nu$(NH)	32(33)	27(85)	19(65)	22(70)	35(96)
	δr(OC)	0.0013	0.0004	0.0007	0.0006	0.0008
	$\delta\nu$(CO)	-12(176)	-1(45)	-3(43)	-2(40)	-5(70)
	$\delta r(NH)^{CP}$	-0.0014	-0.0010	-0.0006	-0.0004	
	$\delta\nu(NH)^{CP}$	29(35)	22(92)	19(70)	17(78)	

energies of the hydrogen bonding. For the C···H−N H bonds, the order of the interaction energies and 0 K dissociation energies computed by various theoretical levels is the following: MP2/6-311++G(2df,2p) ≈ MP2/ AUG-cc-pVDZ > MP2/6-311++G(d,p) > MP4(SDQ)/6-311++G(d,p) > HF/6-311++G(d,p). For the O···H−N H bonds, MP2/AUG-cc-pVDZ and MP2/6-311++G(2df,2p) also predict the largest energies if neglecting the Hartree−Fock method. The CP-corrected gradient technique is of great importance to accurate interaction energies and improves the energy greatly; for the C···HN and O···HN complexes, the improvement of the dissociation energies at the MP2/AUG-cc-pVDZ level is 0.4−0.7 kJ/mol. So, the three factors, a post-HF theory including electron correlation, a high-quality basis set, and the CP-corrected gradient technique, play important roles on predicting an accurate interaction energy for the C(O)···HN H bond (for the triple split valance 6-311G basis set, high angular momentum polarized functions are necessary).

It must be clarified that in Table 2 the interaction energies δE and δE^{CP}, and the dissociation energies D_0 and D_0^{CP}, include the BSSE corrections. Two kinds of methods are used to treat the BSSE. One is that the geometry of the complex is optimized by the use of the standard gradient technique; thereafter a calculation of single point energy is performed to obtained the BSSE correction. Another is that the geometry of the complex is optimized by the use of the CP-corrected gradient technique, and the BSSE correction is obtained directly from the output of the geometry optimization. In Table 2, δE and D_0 are obtained by the use of the standard gradient technique, and δE^{CP} and D_0^{CP} are obtained by the use of the CP-corrected gradient technique; all of them include the BSSE corrections. Here we find that δE^{CP} and D_0^{CP} are always larger than δE and D_0, respectively, which is not in contradiction to the statement in the end of the first paragraph of this section because the geometry obtained by the use of the standard gradient techniques does not include the BSSE correction, but the CP-corrected gradient technique introduces directly the BSSE correction into the optimized geometry of the complex. Table 2 shows that δ(BSSE) is always larger than $\delta(BSSE)^{CP}$, which implies that the first method overcorrects the basis set superposition error, and δ(ZPE) is always larger than $\delta(ZPE)^{CP}$; these results can successfully account for δE^{CP} and D_0^{CP} always being larger than δE and D_0.

Because the dissociation energies of the four O···HN complexes are very small (<3 kJ/mol), even negative for CO···HNO at the MP2 and MP4(SDQ) levels of theory with the 6-311++G(d,p) basis set, a problem occurs whether they can stably exist or not. A calculation at higher levels of theory and with larger basis sets is required. Our results of calculation show that three factors can improve the interaction energies: (1) large basis sets: the dissociation energies at the MP2/6-311++G(2df,2p) level is 0.6∼1kJ/mol larger than those at the MP2/6-311++G(d,p) level for the four O···HN complexes; (2) high theoretical methods: for the two computed complexes CO···HNF_2 and CO···HNO, D_0 at MP4(SDQ)/6-311++G(d,p) is 0.75 and 0.14 kJ/mol larger than at MP2/6-311++G(d,p), respectively; (3) the CP-corrected gradient method: D_0^{CP} are always larger than D_0, as shown above. So, we can believe that the four O···H−N complexes can stably exist at higher levels of theory and with larger basis sets.

3.2. Vibrational Analysis. The experimental vibrational frequency[18] of CO is 2170.21 cm^{-1}. Table 3a shows that the MP2 and MP4(SDQ) methods with the basis sets 6-311G plus polarized and diffuse functions predict a CO stretch frequency near the experimental value, underestimating 20−50 cm^{-1}, the MP2/AUG-cc-pVDZ level underestimates 100 cm^{-1}, and the HF theory overestimates 260 cm^{-1}. So, at an expense of not very large CPU time, the MP2/6-311++G(d,p) method is reliable for the vibrational frequency.

TABLE 4: Results of NBO Analysis at the MP2/6-311++G(d,p) Level: EDT between the Proton Accepter and the Donor; the Variations of the Natural Atomic Charges at Various Atoms, Orbital Occupancies, and *s* Character of Hybrids of N in σ(N−H) on Complexation

properties	OC···HNF_2	OC···$H_2NF(C_1)$	OC···$H_2NF(C_s)$	OC···HNO
δq(N)	−0.01609(0.2557)	−0.00549(−0.31737)	−0.00097	−0.00130(0.03448)
δq(H)	0.01493(0.3197)	0.00946(0.32242)	0.00185	0.01160(0.26031)
δq(X)	−0.00878(−0.2877)	−0.00440(−0.32746)	−0.00384	−0.01034(−0.2948)
δq(C)	−0.02196(−0.59966)	−0.01417	−0.01643	−0.01591
δq(O)	0.03189(0.59966)	0.01608	0.01753	0.01596
EDT	0.00993	0.00191	0.00110	0.00005
$\delta\{\sigma$(N−H)$\}$	0.00020	−0.00032	−0.00076	−0.00048
$\delta\{\sigma^*$(N−H)$\}$	**0.00813**{0.01028}	**0.00252**{0.00337}	0.00014	**0.00160**{0.00239}
$\delta\{\sigma^*$(N−X)$\}$	−0.00156	−0.00006	**0.00261**{0.00310}	−0.00010
δ\{LP(X)\}	0.00182	−0.00086	−0.00051	−0.00102
δ\{LP(C)\}	−**0.01069**{−0.01319}	−**0.00341**{−0.00439}	−**0.00300**{−0.00345}	−**0.00356**{−0.00463}
δs%	1.44%{1.69%}	0.63%{0.78%}	−0.02%	0.60%{0.71%}
E	5.73{7.31}	1.58{2.13}	<0.05	1.55{2.12}

properties	CO···HNF_2	CO···$H_2NF(C_1)$	CO···$H_2NF(C_s)$	CO···HNO
δq(N)	−0.00386	−0.00199	0.00111	−0.00171
δq(H)	0.00957	0.00730	0.00360	0.00941
δq(X)	−0.00546	−0.00341	−0.00513	−0.00708
δq(O)	−0.03158	−0.02027	−0.02358	−0.02345
δq(C)	0.03131	0.01990	0.02399	0.02284
EDT	−0.00027	−0.00037	0.00041	−0.00061
$\delta\{\sigma$(N−H)$\}$	−0.00035	−0.00031	−0.00080	−0.00040
$\delta\{\sigma^*$(N−H)$\}$	0.00003	0.00004	0.00000	−0.00071
$\delta\{\sigma^*$(N−X)$\}$	−0.00072	−0.00002	0.00087	−0.00005
δ\{LP(X)\}	−0.00024	−0.00057	−0.00032	0.00005
δ\{LP(O)\}	−0.00042	−0.00015	−0.00049	−0.00015
δs%	0.37%	0.23%	0.01%	0.33%
E	0.36	0.10	<0.05	0.15

[a] LP(O,C) is the lone pair orbital at oxygen and carbon of CO, LP(X) (X = F, O) is the lone pair orbital at fluorine and oxygen of the proton donors. *E* is the interaction energy of the LP(C, O) and σ^*(N−H) antibonding orbitals (in units of kcal/mol). The values in the parentheses are the natural atomic charges of the monomers, and the values in the brackets are the results for the C···HN complexes at the mp2/6-311++G(2df,2p) level.

Table 3a and b shows that the vibrational harmonic frequencies of the monomers and the complexes computed by the MP2/6-311++G(d,p), MP2/6-311++G(2df,2p), and MP4(SDQ)/6-311++ G(d,p) methods are close to each other. The HF/6-311++G(d,p) method produces larger values and the MP2/AUG-cc-pVDZ method smaller. The different gradient techniques have little influence on the vibrational harmonic frequencies of the complexes; the differences of the frequencies predicted by the two gradient techniques are usually less than 5 cm^{-1}.

The calculation at all of the theoretical levels and using the two optimization methods shows that the formation of the O···H−N H bond causes shortening of the N−H bond of the proton donor with a concomitant blue shift of the N−H stretch vibrational frequency.

The C···H−N H bonds are complicated. In the two complexes, OC···$H_2NF(C_s)$ and OC···HNO, the NH bond is shortening with a blue shift of the NH stretch frequency at all of the theoretical levels. However, in OC···HNF_2 and OC···$H_2NF(C_1)$, HF/6-311++G(d,p) and MP2/ 6-311++G(d,p) produce blue-shifting H bonds, but MP2/6-311++G(2df,2p) and MP2/AUG-cc-pVDZ produce red-shifting H bonds. Thus, we can conclude that in these two complexes red-shifting hydrogen bonds are formed at higher theoretical levels and with larger basis sets. The frequency shifts are less than 10 cm^{-1} for OC···$H_2NF(C_s)$, and 30−40 cm^{-1} for OC···HNO. $\delta\nu$(NH) is positive correlation with δr(NH), which are 0.0016 Å in OC···HNO, and 0.0002 Å in OC···$H_2NF(C_s)$, respectively, at the MP2/6-311++G(d,p). This correlation of bond contraction and frequency shifts is also found in the four blue-shifting O···H−N H bonds. However, the frequency shift and decrease of bond lengths have no correlation with the interaction energies. This circumstance shows that the blue-shifting hydrogen bond is more complicated and difficult than the red-shifting hydrogen bond.

It is worthy of note that the variation of frequency and bond length of CO on the formation of the two types of C···H−N and O···H−N H bonds is different. The calculation at all of the theoretical levels shows that the formation of the C···H−N H bonds causes a large contraction of CO bond length, a blue shift of the CO stretch frequency, and a decrease of the IR intensity, $\delta r = -0.0009$ to -0.0019 Å, $\delta\nu = +6$ to $+15$ cm^{-1}, and $\delta I = -2$ to -9km/mol at the MP2/6311++G(d,p) level, but the formation of the O···H−N H bonds causes a small increase of CO bond length and a small red-shift of CO stretch frequency and increase of the IR intensity, $\delta r = +0.0004$ to $+0.0008$ Å, $\delta\nu = -1$ to -3 cm^{-1}, and $\delta I \approx +10$ km/mol at the MP2/ 6311++G(d,p) level. The magnitude of the variation of CO is consistent with the interaction strength of these two kinds of H bonds: the C···H−N H bonds are stronger than the O···H−N H bonds, and the variation of CO in the former is larger than that in the latter. The red-shifting or blue-shifting character of the CO stretch vibration in the two types of H bonds can be explained by the NBO analysis in the following subsection.

An interesting case occurs in the IR intensity of the N−H stretch vibration. Hermansson[20] proposed that the classical red-shifting H bond is characteristic not only of elongation of X−H bond and a concomitant decrease of its stretch frequency but also of an increase of the IR intensity of the X−H stretch vibration, and that the improper blue-shifting H bond is characterized not only by shortening of the X−H bond and a concomitant increase of its stretch frequency but also by a decrease of the IR intensity of the X−H stretch vibration. But

now we find exceptions of the blue-shifting H bonds. In our blue-shifting H-bonding complexes, the variation trends of IR intensities of the N−H stretch vibration are different. For the proton donor HNO, the IR intensity decreases on complexation as observed by Hermansson, but for the donors HNF_2 and H_2NF containing fluorine, the IR intensities of the N−H stretch modes increase unusually on complexation. This property is also found in the C−H···π blue-shifting H bond in pyridine-$CHCl_3$.[21] We shall discuss this point in detail below.

3.3. Relationship between the Permanent Dipole Moment Derivative of the Proton Donor and the Blue-Shifted and Red-Shifted H Bonds. When the proton donor approaches the acceptor with rich electron density, the electrostatic and polarization interaction, electronic exchange overlap repulsion, and so forth play roles in formation of H bonds. To explain the physical origin of blue-shifting H bonds, Hermansson[20] developed an electrostatic model to investigate the effects of electrostatic field of the proton acceptor on length of the X−H bond, frequency, and IR intensity of the X−H stretch mode. She took a weak electric field, $F_{||}$, directed along the vibrating XH bond, approximate to the field of the proton acceptor, acting on the proton donor, and deduced the following formula:

$$\Delta\upsilon \propto -F_{||}(\mathrm{d}\mu^0/\mathrm{d}r_{XH} + (1/2)\mathrm{d}\mu^{ind}/\mathrm{d}r_{XH}) \qquad (2)$$

Here $\Delta\upsilon$ is the shift of the X−H stretch vibrational frequency, $\mathrm{d}\mu^0/\mathrm{d}r_{XH}$ the permanent dipole moment derivative with respect to the X−H stretch vibrational coordinate of the proton donor, and $\mathrm{d}\mu^{ind}/\mathrm{d}r_{XH}$ the induced dipole moment derivative on complexation. Because $\mathrm{d}\mu^{ind}/\mathrm{d}r_{XH}$ is always positive, Hermanssion concluded that whenever $\mathrm{d}\mu^0/\mathrm{d}r_{XH}$ is positive, the formed X−H···Y hydrogen bond is always red-shifting, and if $\mathrm{d}\mu^0/\mathrm{d}r_{XH}$ is negative, then both red-shifting and blue-shifting H bonds can be formed; which type of H bond is formed is determined by the magnitude of $\mathrm{d}\mu^{ind}/\mathrm{d}r_{XH}$, that is, the intensity of the proton acceptor. A further conclusion is that a negative permanent dipole moment derivative with respect to the X−H stretch vibration coordinate of the proton donor is a necessary (but not sufficient) condition for the formation of a blue-shifting H bond.

Because the IR intensity is proportional to the square of the total dipole moment derivative of the complex, that is

$$I \propto |\mathrm{d}\mu/\mathrm{d}r_{XH}|^2 = |\mathrm{d}\mu^0/\mathrm{d}r_{XH} + \mathrm{d}\mu^{ind}/\mathrm{d}r_{XH}|^2 \qquad (3)$$

According to the above conclusion of Hermansson, whenever the red-shifted H bond is formed, the IR intensity of the X−H stretch vibration always increases, and whenever the blue-shifted H bond is formed, the IR intensity of X−H stretch vibration always decreases. McDowell[22−24] investigated the H-bonding systems containing argon such as N_2···HArCl and demonstrated the above conclusion.

In our work on the formation of the blue-shifted H bonds CO···HNF_2, CO···H_2NF, and OC···$H_2NF(C_s)$, the IR intensity of the N−H stretch vibration increases. To explore the intrinsic origin of this phenomenon, we computed the permanent dipole moments of the proton donors and total dipole moments of all eight complexes at the N−H bond lengths changing from r_e(N−H) − 0.05 Å to r_e(N−H) + 0.05 Å with spacing 0.01 Å (the other parameters are fixed in the equilibrium values), and the permanent dipole moment derivatives with respect to the N−H stretch vibration of the proton donors and the total dipole moment derivatives of the complexes at the MP2/6-311++G(d,p) level, where the MP2 electron density is taken to compute the dipole moment. The results are plotted in Figure 2, where

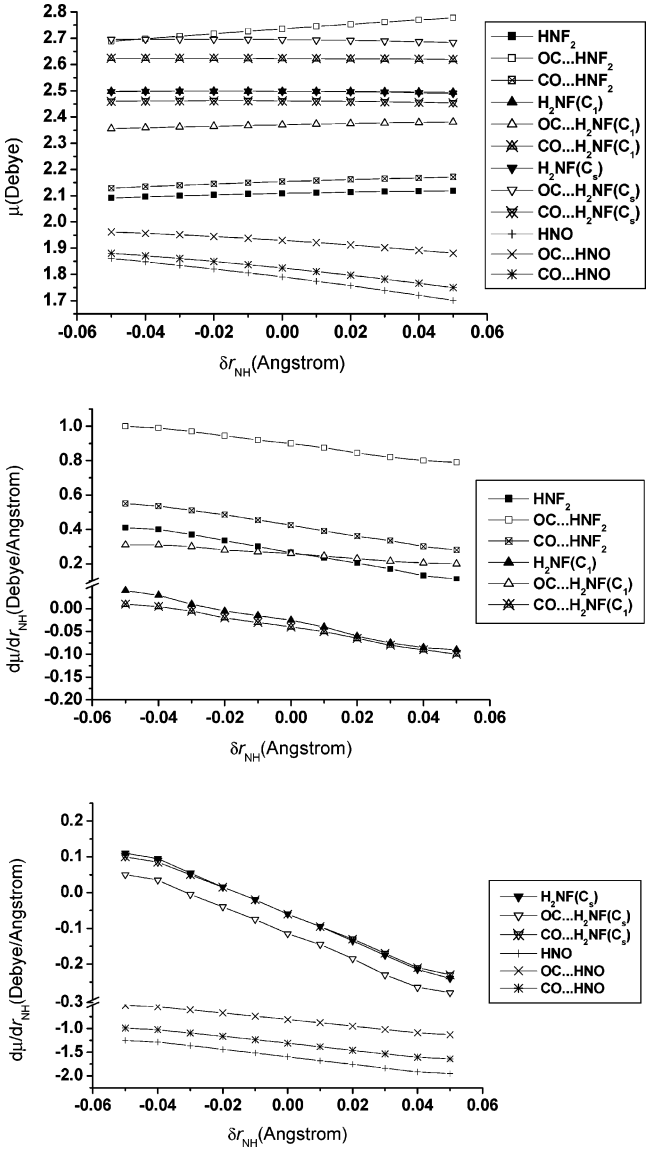

Figure 2. Dipole moments of the proton donors and the eight complexes vs r_{NH} and their derivatives with respect to the N−H stretch vibration at the MP2/6-311++G(d,p) level.

δr_{NH} is the deviation of the N−H bond length from its equilibrium value. From it, we find the following: (1) The dipole moments of OC···HNF_2 and CO···HNF_2 are larger than that of HNF_2, they increase with increasing N−H bond length, and the permanent dipole moment derivative and induced dipole moment derivative are all positive. The dipole moment derivatives of HNF_2, OC···HNF_2, and CO···HNF_2 are 0.27, 0.9, and 0.43 D/Å, respectively, at the equilibrium geometry, so the IR intensity of the NH stretch vibration increases on complexation. (2) The dipole moments of OC···HNO and CO···HNO are larger than that of HNO, they decrease with increasing N−H bond length, the permanent dipole moment derivatives are negative, and the induced dipole moment derivative is positive. The dipole moment derivatives of HNO, OC···HNO, and CO···HNO are −1.6, −0.8, and −1.3 D/Å, respectively, at the equilibrium geometry, so the IR intensity of the NH stretch vibration decreases on complexation. (3) The dipole moment derivatives of $H_2NF(C_1)$ and $H_2NF(C_s)$ are obtained by changing the one or two N−H bonds that are involved in hydrogen bonding; the dipole moment derivatives of the corresponding H-bonding complexes are similarly computed. Figure 2 shows that the results are quite odd. Near the equilibrium geometry,

the permanent dipole moment derivatives are negative; but except for the fact that the induced dipole moment derivative of OC···$H_2NF(C_1)$ is positive the induced dipole moment derivative of CO···$H_2NF(C_s)$ is about zero, and the induced dipole moment derivatives of CO···$H_2NF(C_1)$ and OC···$H_2NF(C_s)$ are negative. The dipole moment derivatives of $H_2NF(C_1)$, OC···$H_2NF(C_1)$ and CO···$H_2NF(C_1)$, and $H_2NF(C_s)$, OC···$H_2NF(C_s)$ and CO···$H_2NF(C_s)$ are −0.025, 0.26, and −0.04, and −0.06, −0.115, and −0.06 D/Å, respectively. Therefore, the IR intensity of the NH stretch vibration always increases on complexation.

Because the H bonds in all eight complexes are blue-shifting at the MP2/6-311++G(d,p) level, according to the above discussion, we obtain two conclusions: (a) A negative permanent dipole moment derivative of the proton donor is not a necessary condition for the formation of a blue-shifted H bond; a donor possessing a positive permanent dipole moment derivative can also form a blue-shifted H bond. The conclusion of Hermansson is not correct because its based formula (2) contains mainly electrostatic interaction; the electronic exchange overlap repulsive interaction in the short range is not included, which is more important in the equilibrium distance between the monomers. McDowell and Buckingham[25] have also found this case in studying the blue-shifted H bonds BF···HCl and CO···HCl, where HCl has a positive permanent dipole moment derivative, and drawn the same above conclusion. (b) Upon formation of a hydrogen bond, the induced dipole moment derivative of the proton donor is not necessarily always positive, here CO···$H_2NF(C_1)$ and OC···$H_2NF(C_s)$ are examples. This is a very unusual and odd result, and we shall further study this problem in detail.

From the above analysis, we obtain several cases: (a) When a proton donor possesses a positive permanent dipole moment derivative and usually a positive induced dipole moment derivative, whenever a red-shifted or blue-shifted H bond is formed, the IR intensity of the XH stretch vibration always increases, such as OC(CO)···HNF_2. (b) When a proton donor possesses a negative permanent dipole moment derivative and usually a positive induced dipole moment derivative, both red-shifted and blue-shifted H bonds can be formed. If $d\mu^{ind}/dr_{XH}$ is small compared to $d\mu^0/dr_{XH}$, then the IR intensity decreases, such as OC(CO)···HNO; if $d\mu^{ind}/dr_{XH}$ is large compared to $d\mu^0/dr_{XH}$, then the IR intensity will increase, such as OC···$H_2NF(C_1)$. If the formula (2) of Hermansson is acceptable, in the first case, a blue-shifted H bond is formed, and in the second case, a red-shifted H bond is formed. (c) When a proton donor possesses a negative permanent dipole moment derivative and unusually a negative induced dipole moment derivative, if the formula (2) of Hermansson is acceptable, then a blue-shifted H bond is usually formed, and the IR intensity of the XH stretch vibration always increases, such as CO···$H_2NF(C_1)$ and OC···$H_2NF(C_s)$. These conclusions may be taken carefully and need further demonstration.

3.4. NBO Analysis. We performed the natural bond orbital calculation at all of the theoretical levels for the C···HN and O···HN complexes; the results of various theories and basis sets show similar characters, and the values at the MP2/6-311++G(d,p) level are typical and listed in Table 4.

The variation of the natural atomic charges on the formation of H bonds shows a similar trend for all eight complexes. The H atom obtains a small positive charge and the N atom obtains small negative charge; the charge redistribution of the proton donors makes the N−H bond more polarized and easy to form H bonds. The repolarization of the N−H bond is accompanied by an increase (rehybridization) of the *s* character of hybrids of nitrogen in the σ(N−H) orbital, which results in shortening of the N−H bond, as observed by Alabugin et al.[13] In the C···HN complexes, the repolarization of the N−H bond is larger than that in the O···HN complexes; the increase of the *s* character of hybrids of nitrogen in the σ(N−H) orbital of the C···HN complexes is several times larger than that of the O···HN complexes. From the electrostatic view, the electric field of the proton acceptor, which aims at elongating the N−H bond, induces the charge redistribution on the donor; conversely, the acquired additional positive charge at hydrogen and the acquired additional negative charge at nitrogen produce an additional electrostatic attractive interaction that causes shortening of the N−H bond and balances with the force elongating the N−H bond of the electric field of the proton acceptor.

A slightly different case occurs in OC···$H_2NF(C_s)$ and CO···$H_2NF(C_s)$, where the *s* character of nitrogen's hybrids in the σ(N−H) orbital has little variation and rehybridization is very small and can be neglected. Corresponding to this, repolarization is small; even nitrogen obtains a small positive charge in CO···$H_2NF(C_s)$, which diminishes the polarization caused by the acquired positive charge at hydrogen. We observed that this difference of OC(CO)···$H_2NF(C_s)$ from the other complexes can be explained by the contacting orientation of hydrogen bonding: there are actually two C(O)···H−N hydrogen bonds formed in OC(CO)···$H_2NF(C_s)$, but only one in the others, this difference makes the C(O)···H−N H bond in OC(CO)···$H_2NF(C_s)$ more deviating linear configuration than in the other complexes; actually, the CHN(OHN) angle in OC(CO)···$H_2NF(C_s)$ is about 90° as shown in Table 1b and c. We obtain a conclusion that a greatly bent C(O)···H−N hydrogen bond shall inhibit repolarization of the N−H bond and rehybridization of nitrogen in the σ(N−H) orbital and formation of blue-shifting H bonds. In a later article, we will demonstrate and discuss this conclusion in detail.

The charge redistribution in the proton donor is also reflected in an acquired small negative charge at the X(═F, O) atom. An acquired additional negative charge in both the N and the X atoms produces an additional electrostatic repulsive interaction between them and finally results in elongation of the N−X bond and a concomitant red shift of the N−X stretch vibrational frequency.

In the four C···H−N complexes, a large electron density is transferred from the proton acceptor CO to the donor except for the case that in OC···HNO the EDT is small, and the variation of the orbital occupancies is also large. However, in the four O···H−N complexes, the electron density transfer between the monomers and the variation of the orbital occupancies are very small. This difference of the C···H−N and O···H−N complexes is consistent with their different strengths of hydrogen bonding. Although the EDT is small in the O···H−N complexes, the variation direction is worthy of note. Except for CO···$H_2NF(C_s)$, a small electron density is transferred from the proton donor to the acceptor CO, which is very unusual because in general the EDT is from the acceptor to the donor. By checking the occupancy in the valence and Rydberg orbitals, it seems that this EDT is mainly from the valence orbitals, mainly the σ(N−H) bonding orbital, of hydrogen to the oxygen valence orbitals of CO, and the decrease of occupancy in σ(N−H) bonding orbitals may explain this EDT. In CO···H_2NF (C_s), the EDT is from the acceptor to the donor. This difference of the direction of the electron density transfer between the two types of H bonds shows that in CO oxygen is electron-positive and carbon is electron-negative in one hand, and on the other

hand, can account for the different red-shifting or blue-shifting character of CO stretch vibration on the formation of the two types of H bonds.

In the four C···H−N complexes, the variation of the orbital occupancies is much larger than that in the O···H−N complexes. We found that in the three complexes OC···HNF_2, OC···$H_2NF(C_1)$, and OC···HNO a large electron density is transferred from the lone pair orbital of carbon to the σ^*(N−H) antibonding orbital; correspondingly, the energies, E, of the $n(C) \rightarrow \sigma^*$(N−H) interactions are also large. These interaction energies are the second-order perturbation energies in the NBO energetic analysis and obtained by use of the Hartree−Fock density based on the MP2-optimized geometry, which shows the strength of nature−bond−orbital interaction. According to the view of Alabugin,[13] a strong hyperconjugation interaction exists in these three complpexes. This hyperconjugation interaction causes elongation of the N−H bond. However, because the rehybridization in the three complexes is also large and makes contraction of the N−H bond, which kinds of H bonds are formed is determined by competition of hyperconjugation and rehybridization. Table 4 shows that the effects of hyperconjugation and rehybridization increase with enlarging the basis set. The H bond in the complex OC···HNO is always blue-shifting, so the rehybridization is always predominant. However, in the other two complexes, OC···HNF_2 and OC···$H_2NF(C_1)$, the H bonds are blue-shifting at the basis set 6-311++G(d,p) but red-shifting at the larger basis set 6-311++G(2df,2p), which shows that the predominant factor of hyperconjugation and rehybridization varies with the basis sets.

Here we also find a slightly different case in OC···H_2NF (C_s), where the electron density in the lone pair of carbon is transferred not to σ^*(N−H) but to σ^*(N−F); the hyperconjugation interaction is very weak and can be neglected, $E(n(C) \rightarrow \sigma^*(N-H)) < 0.05$ kcal/mol. This case also occurs in CO···$H_2NF(C_s)$, although the hyperconjugation interaction is much smaller. This difference from the other complexes can be accounted for by the same reason that the C···HN hydrogen bond in OC···$H_2NF(C_s)$ is much benter than in the others, which have explained the difference of rehybridization. Therefore, we can conclude that a greatly bent H-bond configuration shall also inhibit hyperconjugation and formation of red-shifting H bonds. We shall discuss this point in detail in a later article. Because both hyperconjugation and rehybridization in a very bent H-bond configuration are very small and can be neglected, they cease to explain the formation of the red-shifting or blue-shifting H bonds in this case. Here for OC···$H_2NF(C_s)$, we observe that the view of Hobza[11] comes into effect. The electron density in the lone pair of carbon is transferred mainly to the σ^*(N−F) antibonding orbital, which leads to structural reorganization of H_2NF and subsequent contraction of the N−H bond and a concomitant blue shift of the N−H stretch frequency.

In the four O···HN complexes, the electron density transfer form n(O) to σ^*(N−H) and the interaction energy $E(n \rightarrow \sigma^*)$ are very small, so hyperconjugation is not obvious. In CO···HNF_2, CO···$H_2NF(C_1)$, and CO···HNO, rehybridization is large; therefore, these H bonds are blue-shifting. We can also explain this result by checking the variation of the orbital occupancies. In the two complexes CO···HNF_2 and CO···$H_2NF(C_1)$, the occupancies in σ(N−H) bonding orbitals decrease and occupancies in σ^*(N−H) antibonding orbitals have little change, which decreases the bond orders of the N−H bond and causes the N−H bond elongating. But this elongating effects is less than the shortening effects of repolarization and rehybridization; ultimately, the N−H bond length decreases. In CO···HNO, although the occupancies both in the σ(N−H) bonding orbital and in the σ^*(N−H) antibonding orbital decrease, but the decrease in the latter is larger, this effect makes the N−H bond shorten, which reinforces the effects of shortening by repolarization and rehybridization. So, the contraction of the N−H bond length in CO···HNO is the largest in these four complexes. In the complex CO···$H_2NF(C_s)$, a small electron density is transferred from the lone pair orbital of oxygen to σ^*(N−F), which results in structural reorganization of the donor and shortening of N−H as observed by Hobza.

4. Conclusions

In the literature, the investigation about the blue-shifting H bonds concentrates on the type of C−H···Y and several theoretical studies show that non-carbon-centered blue-shifting H bonds exist, such as HF···HNF_2. Alabugin and co-workers[13] have studied the H bonds between the proton donor HNF_2 and the acceptors H_2O, H_2S, and NH_3 and found that they are all red-shifting. In this article, we look for other nitrogen-centered blue-shifting H bonds and study their properties. Using HF, MP2, and MP4(SDQ) methods with 6-311++G(d,p), 6-311++G(2df,2p), and AUG-cc-pVDZ basis sets, we studied the H bonds between the donors HNF_2, H_2NF, and HNO and the acceptor CO and found that most of them are blue-shifting H bonds at all of the theoretical levels except for OC···HNF_2 and OC···$H_2NF(C_1)$, which are red-shifting at high levels of theory and with large basis sets. Different theoretical methods and basis sets have obvious effects on the geometry structures, interaction energies, and vibrational harmonic frequencies. We apply both the standard gradient and the CP-corrected gradient techniques to study these H-bonding complexes and find that they have little difference on predicting intramolecular geometry parameters and virational frequencies, but the CP-corrected gradient techniques enlarges the C(O)···H distances and the C(O)···H−N angles and improves the H-bonding energy greatly.

The fact that upon formation of the blue-shifting H bonds the IR intensity of the N−H stretch vibration increases unusually for the donors HNF_2 and H_2NF, whereas the IR intensity decreases for the donor HNO as usual, reveals the subtle intrinsic origin of the blue-shifting H bonds. We studied this difference and led to the conclusion that a negative permanent dipole moment derivative of the proton donor is not a necessary condition for the formation of the blue-shifting H bond, and the donor possessing a positive permanent dipole moment derivative can also form a blue-shifting H bond.

Alabugin and co-workers[13] proposed that all H bonds including both red-shifting and blue-shifting H bonds can be explained by the two concepts: hyperconjugation and rehybridization. In our work, from the fact that on the formation of OC(CO)···$H_2NF(C_s)$ the s character of hybrids of nitrogen in the σ(N−H) orbital has little change and the n(C,O) $\rightarrow \sigma^*$(N−H) hyperconjugation interaction is very weak and can be neglected, we conclude that a greatly bent H-bond configuration shall inhibit both rehybridization and hyperconjugation. We found that in the case of a very bent H-bond configuration the concepts of hyperconjugation and rehybridization will cease to explain the formation of the red-shifting and blue-shifting H bonds in this case, and that other concepts are required; for example, the explanation of Hobza may be useful for the blue-shifting H bonds. Although the proton donor is the same HNF_2, the H bonds with the acceptors H_2O, H_2S, NH_3, and OC are red-shifting, but those with HF and CO are blue-shifting, according to Alabugin, the reason is that H_2O, H_2S, NH_3, and OC are strong hyperconjugative donors, but HF and CO

relatively weak hyperconjugative donors, our calculated results about $OC(CO)\cdots HNF_2$ demonstrate this view.

References and Notes

(1) Scheiner, S. *Hydrogen Bonding*; Oxford University Press: New York, 1997.

(2) Jeffrey, G. A. *An Introduction to Hydrogen Bonding*; Oxford University Press: New York, 1997.

(3) Desiraju, G. R.; Steiner, T. *The Weak Hydrogen Bond*; Oxford University Press: Oxford, 1999.

(4) Budesinsky, M.; Fiedler, P.; Arnold, Z. *Synthesis* **1989**, 858.

(5) Boldeskul, I. E.; Tsymbal, I. F.; Ryltsev, E. V.; Latajka, Z.; Barnes, A. *J. Mol. Struct.* **1997**, *436*, 167.

(6) Hobza, P.; Spirko, V.; Havlas, Z.; Buchhold, K.; Reimann, B.; Barth, H.-D.; Brutschy, B. *Chem. Phys. Lett.* **1999**, *209*, 180.

(7) Reimann, B.; Buchhold, K.; Vaupel, S.; Brutschy, B.; Havlas, Z.; Hobza, P. *J. Phys. Chem. A.* **2001**, *105*, 5560.

(8) Delanoye, S. N.; Herrebout, W. A.; van der Veken, B. *J. Am. Chem. Soc.* **2002**, *124*, 11854−11855.

(9) Hobza, P.; Spirko, V.; Selzle, H. L.; Schlag, E. W. *J. Phys. Chem. A* **1998**, *102*, 2501.

(10) Hobza, P.; Havlas, Z. *Chem. Phys. Lett.* **1999**, *303*, 447.

(11) Hobza, P.; Havlas, Z. *Chem. Rev.* **2000**, *100*, 4253.

(12) Li, X.; Liu, L.; Schlegel, H. B. *J. Am. Chem. Soc.* **2002**, *124*, 9639.

(13) Alabugin, I. V.; Manoharan, M.; Peabody, S.; Weinhold, F. *J. Am. Chem. Soc.* **2003**, *125*, 5973.

(14) Gu, Q. Y.; Lou S. C. *Table of Chemical Materials*; Jiangsu Science and Technology Press: P R China, 1998.

(15) Frisch, M. J.; Trucks, G. W.; Schlegel, H. B.; Scuseria, G. E.; Robb, M. A.; Cheeseman, J. R.; Montgomery, J. A., Jr.; Vreven, T.; Kudin, K. N.; Burant, J. C.; Millam, J. M.; Iyengar, S. S.; Tomasi, J.; Barone, V.; Mennucci, B.; Cossi, M.; Scalmani, G.; Rega, N.; Petersson, G. A.; Nakatsuji, H.; Hada, M.; Ehara, M.; Toyota, K.; Fukuda, R.; Hasegawa, J.; Ishida, M.; Nakajima, T.; Honda, Y.; Kitao, O.; Nakai, H.; Klene, M.; Li, X.; Knox, J. E.; Hratchian, H. P.; Cross, J. B.; Bakken, V.; Adamo, C.; Jaramillo, J.; Gomperts, R.; Stratmann, R. E.; Yazyev, O.; Austin, A. J.; Cammi, R.; Pomelli, C.; Ochterski, J. W.; Ayala, P. Y.; Morokuma, K.; Voth, G. A.; Salvador, P.; Dannenberg, J. J.; Zakrzewski, V. G.; Dapprich, S.; Daniels, A. D.; Strain, M. C.; Farkas, O.; Malick, D. K.; Rabuck, A. D.; Raghavachari, K.; Foresman, J. B.; Ortiz, J. V.; Cui, Q.; Baboul, A. G.; Clifford, S.; Cioslowski, J.; Stefanov, B. B.; Liu, G.; Liashenko, A.; Piskorz, P.; Komaromi, I.; Martin, R. L.; Fox, D. J.; Keith, T.; Al-Laham, M. A.; Peng, C. Y.; Nanayakkara, A.; Challacombe, M.; Gill, P. M. W.; Johnson, B.; Chen, W.; Wong, M. W.; Gonzalez, C.; Pople, J. A. *Gaussian 03*, revision C.02; Gaussian, Inc.: Wallingford, CT, 2004.

(16) Boys, S. F.; Bernardi, F. *Mol. Phys.* **1970**, *19*, 553.

(17) Glendening, E. D.; Badenhoop, J. K.; Reed, A. E.; Carpenter, J. E.; Bohmann, J. A.; Weinhold, F. *GenNBO5.0W*; Theoretical Chemistry Institute, University of Wisconsin, Madison WI, 1996−2001.

(18) McHale, J. L. *Molecular Spectroscopy*; Science Press: Beijing, 2003.

(19) Gao S. L., Song J. F. *Manual of Properties of Inorganic Compounds*, translated from Russian; Shanxi Science and Technology Press: P R China, 1983.

(20) Hermansson, K. *J. Phys. Chem.* **2002**, *106*, 4695.

(21) Li, A. Y.; Wang, S. W.; Tan, H. W. *Sci. China, Ser. B*, submitted for publication, 2006.

(22) McDowell, S. A. C. *J. Chem. Phys.* **2003**, *118*, 7283.

(23) McDowell, S. A. C. *J. Mol. Struct.: THEOCHEM* **2003**, *625*, 243.

(24) McDowell, S. A. C. *J. Mol. Struct.: THEOCHEM* **2004**, *674*, 227.

(25) McDowell, S. A. C.; Buckingham, A. D. *J. Am. Chem. Soc.* **2005**, *127*, 15515.